JOURNAL OF CATALYSIS 149, 159–170 (1994)

Models for Partially Hydroxylated Silica and Alumina and the Modeling of Metal–Support Interaction of Triosmium Clusters on Silica and Alumina

Leh-Yeh Hsu,* Sheldon G. Shore,*,[1] Linda D'Ornelas,† Agnes Choplin,† and Jean-Marie Basset†

*Department of Chemistry, Ohio State University, Columbus, Ohio 43210, and †Institut de Recherches sur la Catalyse, Laboratoire Propre du CNRS Conventionné a l'Universite Claude Bernard, Lyon I, 2, Avenue Albert Einstein, 69626 Villeurbanne Cedex, France

Received November 5, 1993; revised May 24, 1994

Surface complexes formed from the reactions of $Os_3(CO)_{12}$ with silica and alumina are generally represented as $(\mu\text{–H})(\mu\text{–OSi}\equiv)Os_3(CO)_{10}$ and $(\mu\text{–H})(\mu\text{–OAl}\equiv)Os_3(CO)_{10}$, with a surface oxygen atom bridging two osmium atoms, and as $(\mu\text{–OSi}\equiv)_2Os_3(CO)_{10}$ and $(\mu\text{–OAl}\equiv)Os_3(CO)_{10}$, in which two surface oxygens bridge the same two osmium atoms. These surface complexes have been modeled employing computer graphics techniques. Models for partially hydroxylated silica and γ-alumina have been developed and metal–support interaction between $(\mu\text{–H})Os_3(CO)_{10}$, $Os_3(CO)_{10}$, and local regions of support surfaces have been studied. Van der Waals interaction energies, nonbonded contacts as a function of orientation of the cluster with respect to the surface, and possible relaxation of the cluster have been considered. The results indicate that the $(\mu\text{–H})Os_3(CO)_{10}$ unit appears to bind readily to selected oxygen sites of the silica and alumina with little or no steric restraint. On the other hand, the cluster unit $Os_3(CO)_{10}$ is not readily accommodated on either the silica or alumina surfaces by means of a double-oxygen bridge to two osmium atoms without extreme disruption of the surface or the cluster.

I. INTRODUCTION

Surface organometallic chemistry deals (1) with the preparation and study of organometallic species grafted onto surfaces such as oxides and hydroxylated oxides. Atoms on the relatively rigid surface can function as ligands to the organometallic fragment. Studies of such surface-bound species can provide useful information leading to more detailed knowledge of reactivities of oxide surfaces, a better understanding of the elementary steps of heterogeneously catalyzed reactions, and the preparation of a new generation of well-defined surface-bound catalysts. While a wide variety of techniques have been applied relative to elucidating surface stoichiometry and structures (e.g., IR, Raman, ^1H and ^{13}C NMR, EXAFS, UV, XPS spectroscopies, STEM, mass balances), we are still reduced in many instances to drawing simple stick figures (Fig. 1) when pressed to describe the local environment of the surface-bound organometallic materials. When dealing with oxide and hydroxylated oxide supports, not only the molecular aspects of the organometallic species, but also the mode of binding to the surface and how the organometallic species interacts with the local surface environment of oxygens and hydroxyl groups, must be considered. As an adjunct to experimental surface studies, computer models of organometallic species on surfaces, based on the structures of both molecular analogs and lattice parameters of the oxide, are potentially useful tools in considering steric factors that govern the accommodation of a molecular species on a relatively rigid surface.

Systems that have received appreciable attention involve the surface complexes formed from the reaction of $Os_3(CO)_{12}$ with hydroxylated silica and alumina (2–7). Spectroscopic results (2–7) indicate that a triosmium core binds to a single surface oxygen by bridging two osmium atoms, $(\mu\text{–H})(\mu\text{–O}M\equiv)Os_3(CO)_{10}$ (M = Si, Al) (Fig. 2a). A second arrangement, $(\mu\text{–O}M\equiv)_2Os_3(CO)_{10}$ (M = Si, Al) (Fig. 2b) that involves two surface oxygens bridging two osmium atoms has been considered (5). This second possibility, which does not account for the catalytic results obtained with the supported cluster (2f), is believed to be more likely on alumina than on silica (5), though more recent work favors the single-oxygen-bridge system (3e). How the triosmium cluster can actually fit on these two surfaces is not discerned by the available experimental data. Therefore, it is of interest to us to model surface complexes that would represent these two arrangements to determine if computer modeling can discriminate between them as to the favored arrangements and to gain possible insight as to how the cluster might be accommodated on local sites of hydroxylated silica and alumina surfaces. Ideally, the methodology for answering these questions would involve optimization of the cluster and the oxide surface. Unfortunately such an approach is at present computationally impractical because of the ab-

[1] To whom correspondence should be addressed.

0021-9517/94 $6.00

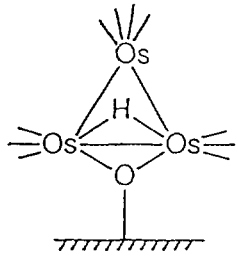

FIG. 1. Typical representation of a cluster bound to an oxide surface.

sence of sufficiently accurate potential parameters and the requirement for overwhelming CPU time, even on the Cray/Y-MP super computer. Therefore, we have chosen an approach that, although qualitative, does identify the most favorable sites for attachment of the cluster and represents a significant advance over the stick figures that are so frequently employed for visualizing the accommodation of clusters on surfaces.

In an earlier report (8), we described preliminary results on our modeling of hydroxylated silica surfaces and their possible interactions with the triosmium cluster species $(\mu\text{-H})Os_3(CO)_3$ and $Os_3(CO)_{10}$. In this report we describe in more detail our development of models for surface sites of hydroxylated silica and hydroxylated alumina. We then consider how the triosmium cluster fragments might fit on the various sites, taking into account nonbonded interactions between cluster atoms and surface atoms through examination of nonbonded contact distances, minimization of the estimated van der Waals interaction energy, and possible relaxation of carbonyl groups.

II. MODELS AND METHODS

A. *Modeling of Hydroxylated Silica*

Although hydroxylated silica is amorphous, evidence indicates local order which resembles that of β-cristobalite and related crystalline phases (9). Studies of hydroxylated silica suggest that the surface is heterogeneous and is probably composed of regions of partially hydroxylated (100) and (111) surfaces, with the degree of hydroxylation being a function of the treatment of the silica (10). Hydroxylation of the (100) surface leads to geminal $Si(OH)_2$ groups (10, 11), which form hydrogen-bonded chains through interaction with neighboring geminal groups (11b,c). Hydroxylation of the (111) surface gives isolated SiOH groups (10, 11). Dehydroxylation of the (100) surface occurs readily to form siloxane bridges (11). On the other hand, dehydroxylation of the (111) plane is unlikely under the conditions in which the surface-bound cluster is formed (10a, 11d). We have derived models for each of these proposed components of the silica surface including defects [edges formed from the intersection of the (100) plane with the (001) plane and the intersection of the (100) plane with the (111) plane].

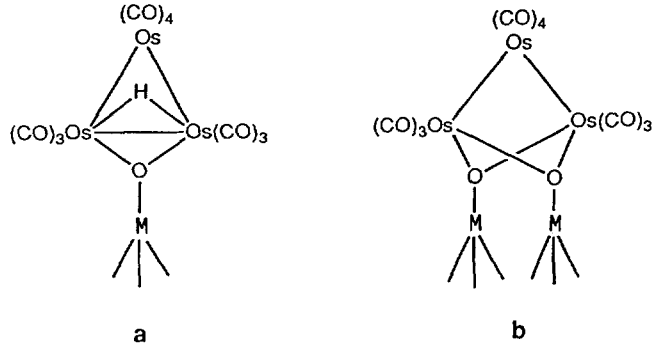

FIG. 2. Representation of (a) $(\mu\text{-H})(\mu\text{-OM}\equiv)Os_3(CO)_{10}$ and (b) $(\mu\text{-OM}\equiv)_2Os_3(CO)_{10}$ (M = Si, Al).

Our models for the surface sites of hydroxylated silica are based on the structure of β-cristobalite. Welberry, Hua, and Withers recently described the structure of β-cristobalite as one in which the oxygen atoms are disordered (12). They are distributed uniformly around an annulus which encircles the 16(c) sites of the *Fd3m* space group. This structure differs from that reported by Wyckoff (13) a number of years ago. The Wyckoff structure is effectively one of the possible structures in the disordered model of Welberry *et al.* (12). While it would be extremely difficult to produce coordinates for models of the cluster on surface sites based on Welberry and colleagues' structure, Wyckoff's (13) structure is satisfactory as the starting point in our modeling procedures. Since the Si atom positions are essentially the same in both structures and since one of our criteria for determining whether a cluster can be accommodated on a surface site is based on the distances between nonbonded contacts of cluster atoms with silica surface atoms, we take into account the oxygen disorder by considering the range of oxygen atom locations around the 16(c) sites in evaluating nonbonded contacts.

1. The (100) surface. Modeling of the local regions on the (100) plane involved first generating, by means of CHEMX (14), a β-cristobalite lattice consisting of 3 × 3 unit cells along the b and c axes (13). A hydroxylated surface was derived by adding hydrogen atoms to these surface oxygens to form geminal silanol groups which were oriented to allow hydrogen-bonded chains consistent with spectroscopic studies (11b,c). The hydrogens were placed on (100) surface oxygens such that the O–H distance was 1.00 Å, and the H–O–Si angle was 109.5°, with the dihedral angles of H–O–Si–O equal to 180.0° and 0°. To reduce dipolar contributions from O–H groups on the surface, the directions of adjacent hydrogen-bonded chains were arranged to minimize such contributions. The final arrangement for hydrogen positions of a fully hydroxylated (100) surface is shown in Fig. 3a.

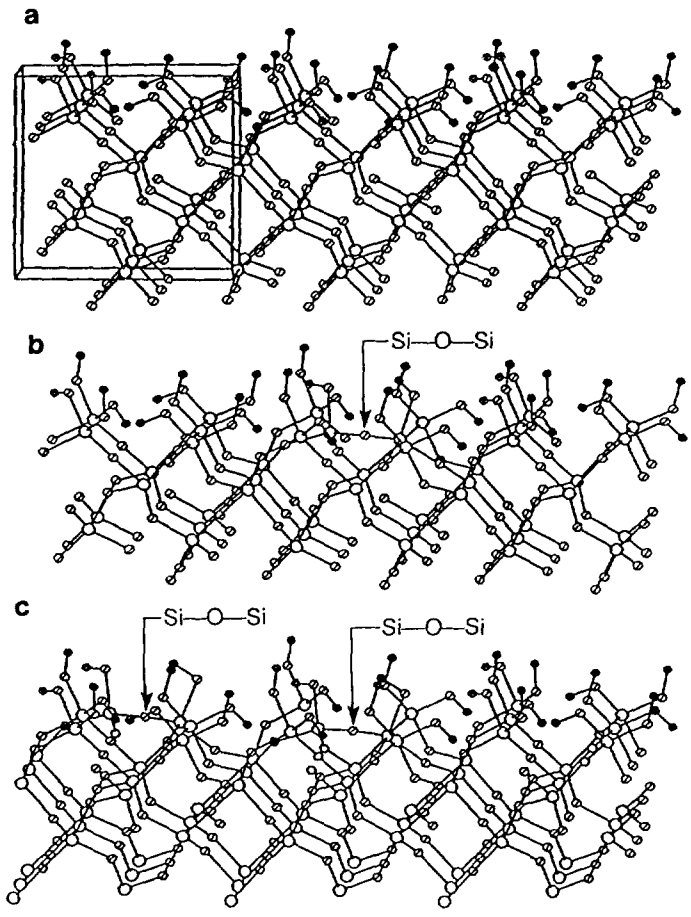

FIG. 3. Models of local surface sites of silica: (a) fully hydroxylated (100) plane, (b) partially hydroxylated (100) plane represented by a Si–O–Si bridge, (c) partially hydroxylated (100) plane represented by two adjacent Si–O–Si bridges.

The following procedure was used to derive a partially dehydroxylated local surface region. An H_2O molecule was removed from the central unit cell of a fully hydroxylated (100) surface (Scheme 1), constructed of 3 × 3 unit cells, thereby leaving an oxygen atom available for bridging between two Si atoms. Then a subset of atoms of the main structure (bridged oxygen, two bonded silicon atoms, two hydroxyl groups, four oxygen atoms, and all of the lone-pair electrons of these oxygens) was optimized (15). Figure 3b shows the optimized structure in which Si–O distances in the siloxane bridge are 1.637 and 1.635 Å and the Si–O–Si angle is 177.2°. The Si–O–Si angle of the isolated siloxane bridge derived here is uncommon, but not unknown (16). For $Sc_2Si_2O_7$ (16b,c), the Si–O–Si angle is 180°, and for $Rb_2Sb_2Si_2O_7$ (16d), the Si–O–Si angle is 171°.

Since experimental results suggest a relatively low concentration of geminal Si(OH) (10b,c) units there is probably a significant concentration of local dehydroxylated

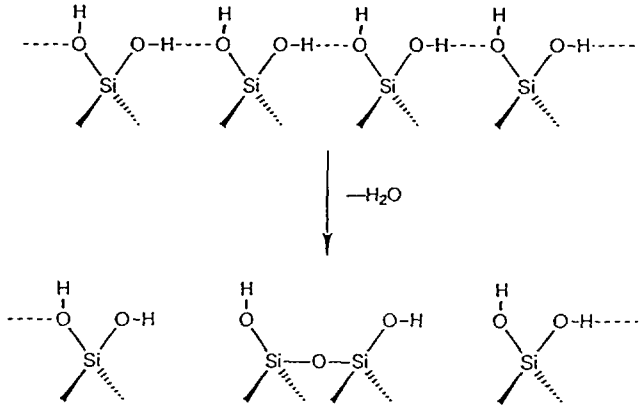

SCHEME 1

surface which contains adjacent siloxane bridges. Such a region was constructed in a manner analogous to that described above by modeling the removal of two H_2O molecules from the fully hydroxylated (100) plane to give two adjacent Si–O–Si bridges (Scheme 2) (Fig. 3c).

2. The (111) surface and intersections of surface planes. To obtain a model of the (111) plane a 3 × 3 × 3 lattice was constructed and then a section was removed by cutting through the (111) intercepts, thereby exposing the (111) plane. In this case there is no hydrogen bonding between the SiOH units because of the large distance of separation between them (ca. 4–6 Å).

Defect sites were also created. Local regions were constructed from the intersection of the (100) and (001) planes and from the intersection of the (100) and (111) planes.

B. Modeling of Hydroxylated Alumina

Based on the pseudomorphosis relations described by Lippens (17, 18) it has been concluded that the preferentially exposed faces of γ-alumina are the (100) face and the C- and D-layers of the (110) planes (19, 20). The hydroxylated alumina surface is considered to be heteroge-

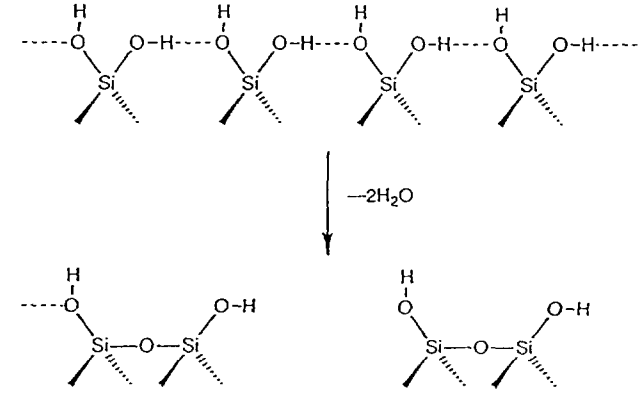

SCHEME 2

neous. It has been described as being composed of local regions which are related to the (100) face, (110) C-layers, and (110) D-layers of hydroxylated γ-alumina. Hydroxylation (19) of the (100) surface leads to a configuration (schematically represented in Fig. 4a) in which the OH group is coordinated to a single cation that resides at an octahedral site. Hydroxylation of the C- and D-layers parallel to the (110) face produces three different configurations (schematically represented in Figs. 4b and c). In the OH layer on top of a C-layer of the (110) plane, two OH configurations occur: (1) a terminal OH group is coordinated to a single tetrahedral Al^{3+} cation, and (2) a bridging OH group links two octahedral Al^{3+} cations. On the other hand, there is only one configuration of the OH group on top of the D-layer. Dehydroxylation (20) of the alumina surface has been postulated to generate "strained oxide linkages" (21), a reaction that may be depicted as

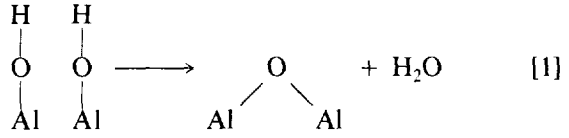

[1]

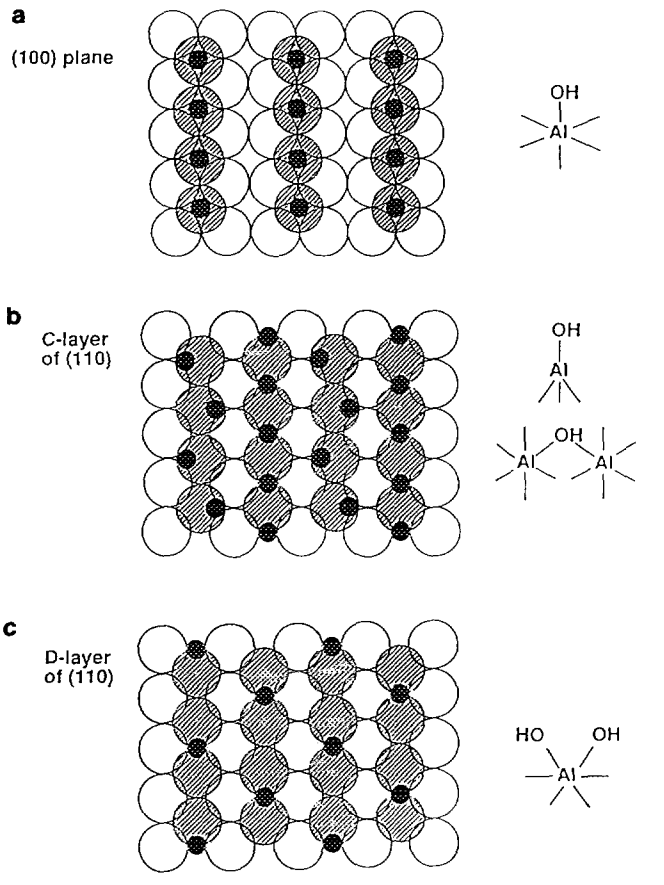

FIG. 4. Representations of local surface sites of hydroxylated γ-alumina.

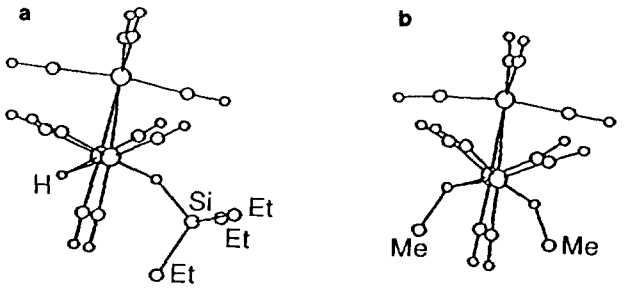

FIG. 5. Molecular structures of (a) $(\mu\text{-H})(\mu\text{-OSiEt}_3)Os_3(CO)_{10}$ and (b) $(\mu\text{-OMe})_2Os_3(CO)_{10}$.

However, it is now agreed (20, 22) that the dehydroxylation process leaves an oxide ion in the outermost surface layer and an exposed incompletely coordinated aluminium ion in the next-lowest layer, as shown by

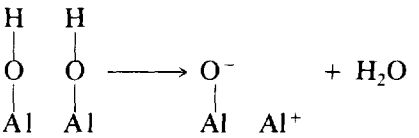

[2]

Our models for the surface sites of partially hydroxylated alumina surface are derived from the structure of γ-alumina (17, 23). This structure is based on the spinel lattice with $21\frac{1}{3}$ aluminum atoms and $2\frac{2}{3}$ vacant aluminum sites distributed over the otahedral and tetrahedral positions (20). Greatest disorder is expected in the tetrahedral positions.

We have modeled, separately, each of the proposed components of hydroxylated alumina surface using the same techniques as described above for hydroxylated silica. Six local arrangements of γ-alumina surfaces were modeled: a fully hydroxylated (100) face of γ-alumina, a fully hydroxylated (110) face C-layer, a fully hydroxylated (110) face D-layer, a partially hydroxylated (100) face, a partially hydroxylated (110) face C-layer, and a partially hydroxylated (110) face D-layer.

C. Modeling Cluster Fragments on Local Regions of Silica and Alumina Surfaces

Summarized below are procedures employed in attempts to fit $(\mu\text{-H})Os_3(CO)_{10}$ and $Os_3(CO)_{10}$ to the local regions of silica and alumina surfaces described above to generate the surface complexes $(\mu\text{-H})(\mu\text{-OSi}\equiv)Os_3(CO)_{10}$, $(\mu\text{-H})(\mu\text{-OAl}\equiv)Os_3(CO)_{10}$, $(\mu\text{-OSi}\equiv)_2Os_3(CO)_{10}$, and $(\mu\text{-OAl}\equiv)_2Os_3(CO)_{10}$. Parameters for the cluster fragments were obtained from X-ray structures of the model compounds $(\mu\text{-H})(\mu\text{-OSiEt}_3)Os_3(CO)_{10}$ (24) and $(\mu\text{-OMe})_2Os_3(CO)_{10}$ (25) (Fig. 5). Flow diagrams for

the computer programs employed in the fitting procedures are given in the supplementary material.[1]

For fitting the $(\mu\text{-H})Os_3(CO)_{10}$ fragment to a local region of the surface, a hydrogen atom was removed from an OH group of a central unit cell of fully hydroxylated (100) surface constructed, as described above, from 3 × 3 unit cells. Then the $(\mu\text{-H})Os_3(CO)_{10}$ fragment was attached to the exposed oxygen in the same manner that the $OSiEt_3$ unit binds this fragment in the complex $(\mu\text{-H})(\mu\text{-OSiEt}_3)Os_3(CO)_{10}$ (24). In the process of fitting the cluster fragment to the surface, the coordinates of the surface O, Si, and Al atoms were always fixed, but the hydrogen atoms, where necessary, were displaced to avoid clashes with the cluster atoms; O–H bond lengths and Si(or Al)–O–H bond angles were unchanged. The $(\mu\text{-H})Os_3(CO)_{10}$ fragment was then rotated about the oxygen of the Si–O bond or the Al–O bond throughout 360° at 3° intervals. The dihedral angle between the Os–O–Os plane and Si (or Al)–O bond was also varied from 154.3° to near 180° at 5.1° intervals. This is equivalent to assuming that the bending force constant for the angle between the Os–O–Os plane and the O–Si (O–Al) bond is small and that the dihedral angle might be opened up to provide a better fit to the surface.

For each orientation of the cluster fragment, the van der Waals nonbonded interaction energy between the cluster and the surface atoms was calculated, summing from the individual cluster atoms all of the interactions with surface atoms up to 6 Å away. The van der Waals nonbonded interaction energy, E_{vdw}, was calculated from the expression

$$E_{vdw} = \varepsilon[-C_1(r^*/r)^6 + C_2 \exp(-C_3(r/r^*))]$$

The constants, C_1, C_2, and C_3 are 2.25, 290,000, and 12.50, respectively. The potential parameters ε and r^* for atom types H, C, O, and Si were obtained from Allinger and Yuh (26). For Al and Os atom types, the ε and r^* were estimated as 0.12 and 2.20 for Al and 0.26 and 2.65 for Os (27). Calculated nonbonded van der Waals interaction energies between the cluster atoms and the surface atoms cannot be considered to be absolute, but are useful for comparing relative stabilities of the different orientations of the cluster with respect to the surface in terms of these approximate relative energies.

Nonbonded contact distances between cluster and surface atoms were monitored at each interval during rotation of the cluster. Criteria for deciding whether a particular surface site could accommodate an $(\mu\text{-H})Os_3(CO)_{10}$ or $Os_3(CO)_{10}$ cluster unit are based on the absence of "short" nonbonded contacts between atoms of the cluster and atoms of the oxide surface.[2]

Where "short" contact distances[2] occurred between the oxygen atom of a carbonyl group and a surface atom, relaxation of that carbonyl group was performed. The relaxation process involved varying the Os–C–O angle from 180° to 165° at 5° intervals. The C–O bond was rotated through 360° about the carbon of the Os–C bond at intervals of 5°, 10°, or 15° depending on the Os–C–O angle (Table 1 and Fig. 6a) and "short" contact distances between the carbonyl oxygen atom and surface atoms were monitored.

Rotations of $Os(CO)_3$ and $Os(CO)_4$ groups were carried out if either "short" contact distances between carbonyl oxygen and surface atoms were not relieved through rotation of the C–O bond around the Os–C bond or "short contact" distances existed between the carbonyl carbon atom and surface atoms. The $Os(CO)_3$ groups were rotated around a vector passing through Os(1) and Os(2), whereas the $Os(CO)_4$ group was rotated around a vector that is the perpendicular bisector of the Os(1)–Os(2) vector (Fig. 6). Rotations were carried out from −15° to +15° in 3° intervals and short contact distances between the carbonyl atoms and surface atoms were monitored. If there were "short contact" distances between a carbonyl oxygen atom and surface atoms, relaxation of that specific carbonyl group would be executed.

Attempts to fit the $Os_3(CO)_{10}$ unit to local regions of the silica and alumina surfaces were similar to the procedures described above except that two hydrogen atoms were removed from two OH groups of the surface. The $Os_3(CO)_{10}$ fragment was then bonded to the two oxygen atoms in the same way as the two OMe units bind this fragment in the complex $(\mu\text{-OMe})_2Os_3(CO)_{10}$ (25) to give

[1] Flow diagrams for computer programs and listings of atomic coordinates of silica and alumina surface sites are available on request from S. G. Shore.

[2] Criteria for "short" nonbonded atom–atom contacts were set smaller than the sum of van der Waal's radii but about equal to the shortest atom–atom nonbonded contacts observed in the crystalline state. Normally, nonbonded atom contact distances are smaller than the sum of van der Waals radii; e.g., the nonbonded oxygen–oxygen contact is 2.42 Å in β-cristabolite. When a metal cluster binds to the oxide surface, the binding force may cause nonbonded contacts to be shorter. Furthermore, oxide surface atoms may relax, in addition to the carbonyl groups of a cluster fragment. Since proper potential parameters are not available for metal cluster atoms and oxide surface atoms, optimization of cluster–surface complex structures using a molecular mechanics approach could not be performed. Therefore, we estimated the threshold of short contact distances as listed below:

Atom–atom contacts	Threshold	Atom–atom contacts	Threshold
O–O	2.40 Å	C–Si	2.95 Å
O–Si	2.68	C–Al	2.60
O–Al	2.40		
C–O	2.60		

TABLE 1

Increments and Ranges of Angles of Rotation in the Relaxation of $(\mu\text{-H})Os_3(CO)_{10}$

Rotation	Angle	Range	Increment
a	Between Os(1)–O–Os(2) plane and O–Si bond	154.3°–179.8°	5.1°
b	Os(1)–O–Si–O(surface)	0.0–357.0°	3.0°
	C(11)–Os(1)–Os(2)–Os(3)		
c	C(12)–Os(1)–Os(2)–Os(3)		
	C(13)–Os(1)–Os(2)–Os(3)		
	C(21)–Os(2)–Os(1)–Os(3)		
c′	C(22)–Os(2)–Os(1)–Os(3)	$D - 15.0° < D < D + 15.0°$	3.0°
	C(23)–Os(2)–Os(1)–Os(3)		
	C(31)–Os(3)–m–Os(1)		
c″	C(32)–Os(3)–m–Os(1)		
	C(33)–Os(3)–m–Os(1)		
	C(34)–Os(3)–m–Os(1)		
d	O(11)–C(11)–Os(1)		
	O(12)–C(12)–Os(1)		
	O(13)–C(13)–Os(1)		
	O(21)–C(21)–Os(2)		
	O(22)–C(22)–Os(2)	165.0–180.0°	5.0°
	O(23)–C(23)–Os(2)		
	O(31)–C(31)–Os(3)		
	O(32)–C(32)–Os(3)		
	O(33)–C(33)–Os(3)		
	O(34)–C(34)–Os(3)		
e	O(11)–C(11)–Os(1)–Os(2)		
	O(12)–C(12)–Os(1)–Os(2)		
	O(13)–C(13)–Os(1)–Os(2)		
	O(21)–C(21)–Os(2)–Os(3)		
	O(22)–C(22)–Os(2)–Os(3)		
	O(23)–C(23)–Os(2)–Os(3)	0.0–345.0°	15.0° (d = 175°)
	O(31)–C(31)–Os(3)–Os(1)	0.0–350.0°	10.0° (d = 170°)
	O(32)–C(32)–Os(3)–Os(1)	0.0–355.0°	5.0° (d = 165°)
	O(33)–C(33)–Os(3)–Os(1)		
	O(34)–C(34)–Os(3)–Os(1)		

the two surface oxygens bridging two Os atoms. With this arrangement, the cluster fragment cannot be rotated with respect to the surface and the dihedral angle between an Os–O–Os plane and the Si–O (or Al–O) cannot be varied. However, where appropriate, carbonyl groups were relaxed.

III. RESULTS AND DISCUSSION

A. Modeling the $(\mu\text{-H})(\mu\text{-OSi}\equiv)Os_3(CO)_{10}$ Surface Complex

Table 2 lists the minimum van der Waals energies and short contact distances between the atoms of $(\mu\text{-H})Os_3(CO)_{10}$ and the local regions of silica surface. For the fully hydroxylated (100) and (111) surfaces the minimum van der Waals interaction energies calculated are 364.1 and 151.1 kcal, respectively. There are a number of unreasonably short nonbonded contact distances between the cluster fragment and surface atoms, thus indicating that these local regions of the surface are not satisfactory for accommodating $(\mu\text{-H})Os_3(CO)_{10}$. Relaxation of $(\mu\text{-H})Os_3(CO)_{10}$ does not improve the fit.

For $(\mu\text{-H})Os_3(CO)_{10}$ on the partially hydroxylated local region of the (100) surface that contains an isolated siloxane group, no short contacts between the cluster atoms and surface atoms were observed after $(\mu\text{-H})Os_3(CO)_{10}$ was relaxed by rotating the $Os(3)(CO)_4$ group 12° from its orientation in the solid-state structure of the model compound $(\mu\text{-H})(\mu\text{-OSiEt}_3)Os_3(CO)_{10}$ (24), and one of the Os–C–O units was bent 10° from linear. The calculated minimum van der Waals interaction energy is 11.6 kcal. For $(\mu\text{-H})Os_3(CO)_{10}$ on the partially hydroxylated local region of the (100) surface with adjacent siloxane groups, the calculated minimum van der Waals interaction energy is 2.4 kcal and no short contacts between the cluster atoms

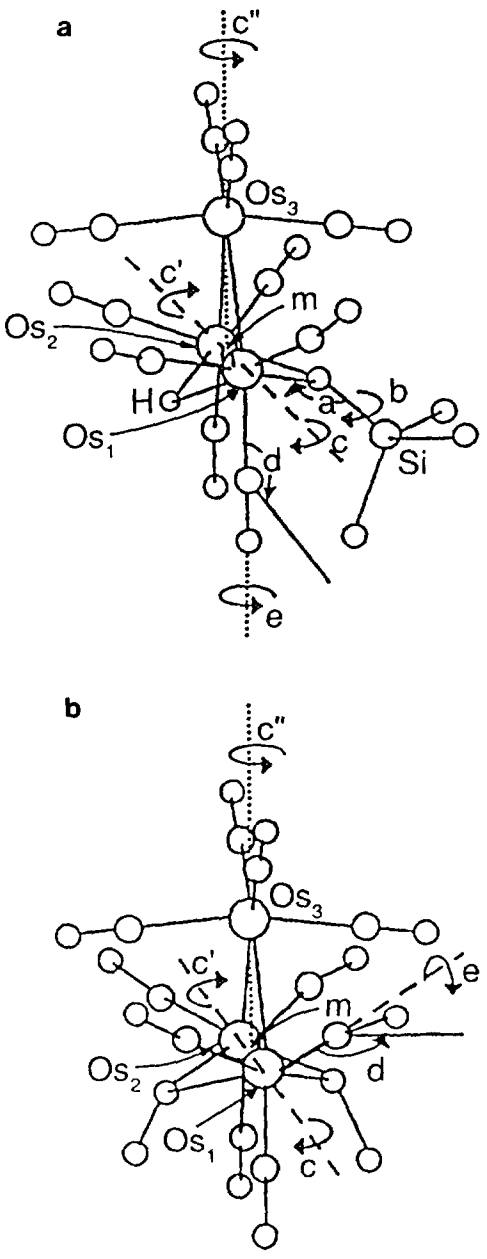

FIG. 6. Bending and rotational relaxation of the clusters (a) $(\mu\text{-H})(\mu\text{-OSiEt}_3)Os_3(CO)_{10}$ and (b) $(\mu\text{-OMe})_2Os_3(CO)_{10}$.

TABLE 2

Van der Waals Energies and Short Nonbonded Distances between $(\mu\text{-H})Os_3(CO)_{10}$ and Local Regions of Silica Surface

Number of short contacts	Range of short contacts (Å)
A. Fully hydroxylated (100) plane, E_{vdw} = 364.1 kcal	
9	$O_{carbonyl}$–$O_{surface}$ 1.481–2.395
3	$O_{carbonyl}$–$Si_{surface}$ 2.176–2.402
2	$C_{carbonyl}$–$O_{surface}$ 1.691–1.804
1	$C_{carbonyl}$–$Si_{surface}$ 2.355
B. Fully hydroxylated (111) plane, E_{vdw} = 151.1 kcal	
5	$O_{carbonyl}$–$O_{surface}$ 1.841–1.965
2	$O_{carbonyl}$–$Si_{surface}$ 1.911–2.030
2	$C_{carbonyl}$–$O_{surface}$ 2.538–2.597
None	$C_{carbonyl}$–$Si_{surface}$ >2.95
C. Partially hydroxylated (100) plane, single siloxane bridge, E_{vdw} = 11.6 kcal	
None	$O_{carbonyl}$–$O_{surface}$ >2.40
None	$O_{carbonyl}$–$Si_{surface}$ >2.68
None	$C_{carbonyl}$–$O_{surface}$ >2.60
None	$C_{carbonyl}$–$Si_{surface}$ >2.95
D. Partially Hydroxylated (100) plane, adjacent siloxane bridges, E_{vdw} = 2.4 kcal	
None	$O_{carbonyl}$–$O_{surface}$ >2.40
None	$O_{carbonyl}$–$Si_{surface}$ >2.68
None	$C_{carbonyl}$–$O_{surface}$ >2.63
None	$C_{carbonyl}$–$Si_{surface}$ >2.95
E. Edge formed from the intersection of (100) plane and (001) plane, E_{vdw} = −3.6 kcal	
None	$O_{carbonyl}$–$O_{surface}$ >2.60
None	$O_{carbonyl}$–$Si_{surface}$ >2.85
None	$C_{carbonyl}$–$O_{surface}$ >2.70
None	$C_{carbonyl}$–$Si_{surface}$ >2.95
F. Edge formed from the intersection of (100) plane and (111) plane, E_{vdw} = 4.9 kcal	
None	$O_{carbonyl}$–$O_{surface}$ >2.40
None	$O_{carbonyl}$–$Si_{surface}$ >2.80
None	$C_{carbonyl}$–$O_{surface}$ >2.60
None	$C_{carbonyl}$–$Si_{surface}$ >2.95

and surface atoms were observed. It was not necessary to relax the carbonyl groups. Thus, the partially hydroxylated (100) silica surfaces which contain isolated and adjacent siloxane groups appear to accommodate the $(\mu\text{-H})Os_3(CO)_{10}$ cluster unit. Figures 7a and b show these arrangements. Note that dehydroxylation leaves a "pocket" on the silica surface into which the $(\mu\text{-HOs}_3(CO)_{10}$ unit can fit.

The defect site created by the intersection of the (100) face with the (001) face readily accommodates $(\mu\text{-H})Os_3(CO)_{10}$ (Fig. 8a). A minimum van der Waals interaction energy of −3.6 kcal was calculated, and no short contacts between the cluster atoms and surface atoms were observed. Relaxation of the cluster carbonyl groups was not necessary.

For the defect site created by the intersection of the (100) and (111) faces it was necessary to relax the $(\mu\text{-H})Os_3(CO)_{10}$ group to achieve a reasonable fit (Fig. 8b). The $Os(CO)_4$ group was rotated 3°, and one of the Os–C–O units was bent 5° from linear. At this conformation the minimum van der Waals energy was 4.9 kcal and no short contacts between the cluster atoms and surface atoms were observed.

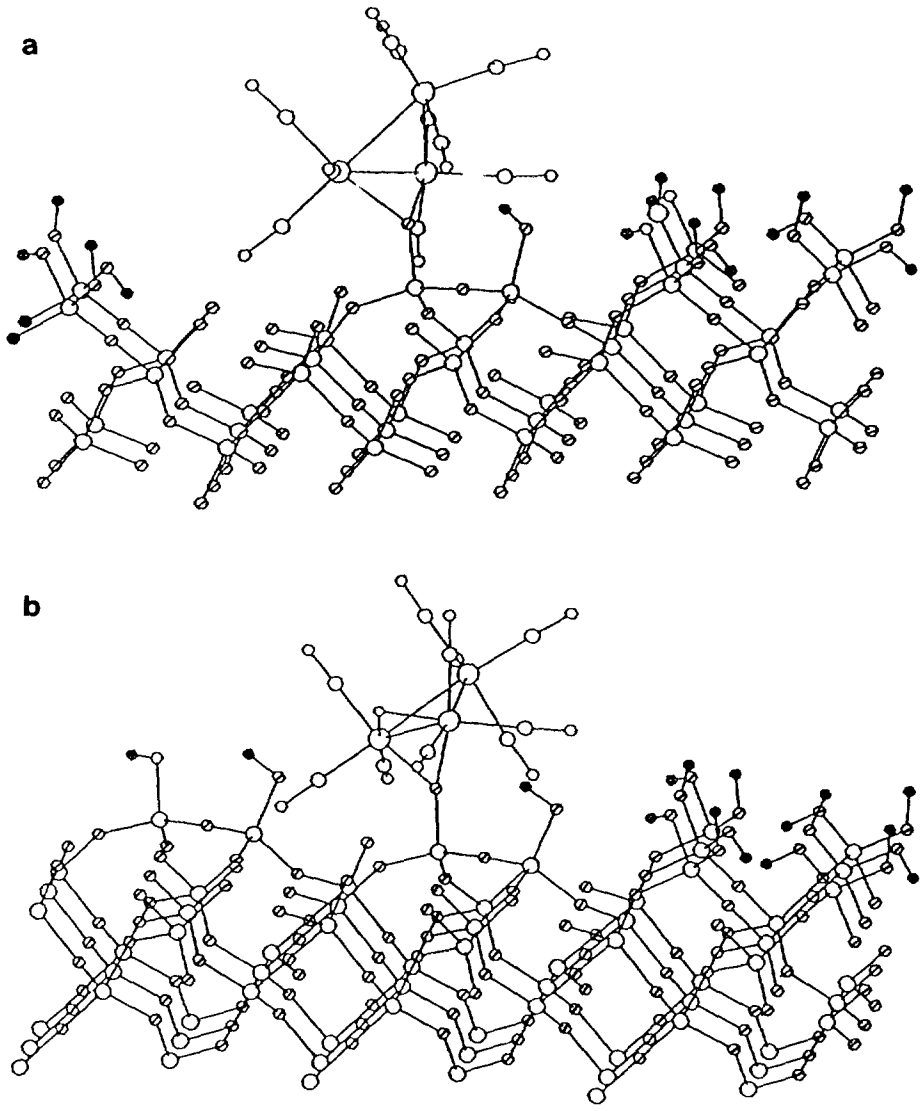

FIG. 7. Models for $(\mu\text{-H})(\mu\text{-OSi}\equiv)Os_3(CO)_{10}$ with $(\mu\text{-H})Os_3(CO)_{10}$ bound to a surface oxygen of a local partially hydroxylated region of the (100) plane containing (a) a single Si–O–Si bridge and (b) adjacent Si–O–Si bridges.

B. Modeling the $(\mu\text{-OSi}\equiv)_2Os_3(CO)_{10}$ Surface Complex

For the fully hydroxylated (100) surfaces, fitting the $Os_3(CO)_{10}$ unit to form a double bridge with surface oxygens results in the axial carbonyls of the cluster being forced beneath the (100) surface (Fig. 9) unless the surface and/or the cluster are very severely disrupted. For the partially hydroxylated (100) local regions and the defect local regions of the (100) silica surface, a double-oxygen bridge cannot be fitted to $Os_3(CO)_{10}$ because of the long distance between available oxygen atoms, 4–6 Å, compared with the observed distance between the bridge oxygen atoms, 2.59 Å, in the model compound $(\mu\text{-OMe})_2Os_3(CO)_{10}$.

C. Modeling the $(\mu\text{-H})(\mu\text{-OAl}\equiv)Os_3(CO)_{10}$ Surface Complex

Table 3 lists the minimum van der Waals energies and short contact distances between atoms of $(\mu\text{-H})Os_3(CO)_{10}$ and the atoms on the surfaces of local regions of γ-alumina. The calculated minimum van der Waals interaction energies are 289.6, 1374.7, 1976.8, and 681.9 kcal, respectively, for the following local regions: fully hydroxylated (100) face, fully hydroxylated (110) face C-layer, fully hydroxylated (110) face D-layer, and partially hydroxylated (110) face C-layer. There are a number of unreasonably short nonbonded contact distances between the cluster atoms and the surface atoms.

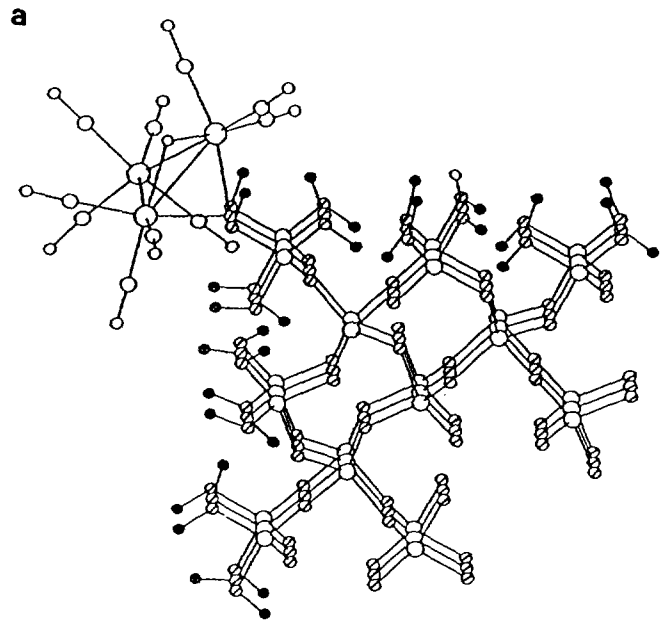

FIG. 8. Models for $(\mu\text{-H})(\mu\text{-OSi}\equiv)Os_3(CO)_{10}$ with $(\mu\text{-H})Os_3(CO)_{10}$ bound to a surface oxygen at the intersection of the (a) (100) and (001) faces and (b) (100) and (111) faces.

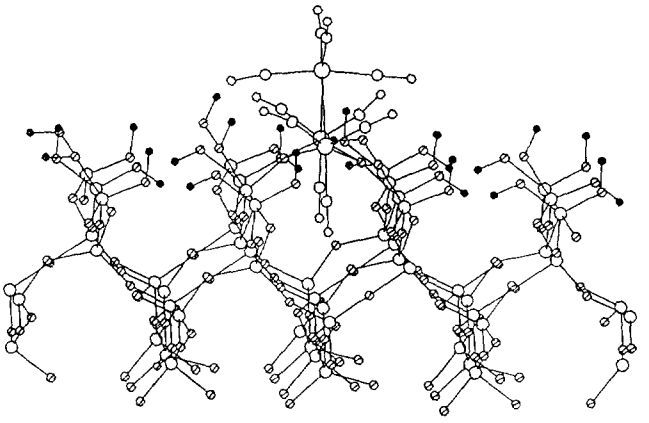

FIG. 9. Models for $(\mu\text{-OSi}\equiv)_2Os_3(CO)_{10}$ with $Os_3(CO)_{10}$ bound to two surface oxygens of the (100) plane. Note the axial carbonyls penetrating the silica surface.

For the local region defined by the partially hydroxylated (100) face, the relaxed $(\mu\text{-H})Os_3(CO)_{10}$ is accommodated without any short contacts (Fig. 10a). The calculated minimum van der Waals interaction energy is 5.3 kcal. In the relaxation procedure the dihedral angle between the Os–O–Os plane and the Al–O bond of the cluster was opened up to 169.6° (model structure is 154.3°) and the $Os(1)(CO)_3$ group was rotated 6°.

For the local region defined by the partially hydroxylated D-layer of the (110) face, the relaxed $(\mu\text{-H})Os_3(CO)_{10}$ is accommodated without any short contacts (Fig. 10b).

TABLE 3

Van der Waals Energies and Short Nonbonded Distances between $(\mu\text{-H})Os_3(CO)_{10}$ and Local Regions of Alumina Surface

Number of short contacts	Range of short contacts (Å)
A. Fully hydroxylated (100) plane, E_{vdw} = 289.6 kcal	
6 $O_{carbonyl}$–$O_{surface}$	1.300–2.391
None $O_{carbonyl}$–$Al_{surface}$	>2.4
2 $C_{carbonyl}$–$O_{surface}$	1.506–1.834
None $C_{carbonyl}$–$Al_{surface}$	>2.6
B. Fully hydroxylated (110) C-layer, E_{vdw} = 1374.7 kcal	
13 $O_{carbonyl}$–$O_{surface}$	1.492–2.264
5 $O_{carbonyl}$–$Al_{surface}$	1.692–1.918
4 $C_{carbonyl}$–$O_{surface}$	1.194–2.025
1 $C_{carbonyl}$–$Al_{surface}$	1.908
C. Fully hydroxylated (110) D-layer, E_{dwv} = 1976.8 kcal	
13 $O_{carbonyl}$–$O_{surface}$	1.101–2.2029
1 $O_{carbonyl}$–$Al_{surface}$	1.812
10 $C_{carbonyl}$–$O_{surface}$	1.023–2.000
2 $C_{carbonyl}$–$Al_{surface}$	1.608–1.996
D. Partially hydroxylated (100) plane, E_{vdw} = 5.3 kcal	
None $O_{carbonyl}$–$O_{surface}$	>2.40
None $O_{carbonyl}$–$Al_{surface}$	>2.40
None $C_{carbonyl}$–$O_{surface}$	>2.40
None $C_{carbonyl}$–$Al_{surface}$	>2.40
E. Partially hydroxylated (110) C-layer, E_{vdw} = 681.9 kcal	
5 $O_{carbonyl}$–$O_{surface}$	1.492–1.971
5 $O_{carbonyl}$–$Al_{surface}$	1.692–1.918
2 $C_{carbonyl}$–$O_{surface}$	2.024–2.141
1 $C_{carbonyl}$–$Al_{surface}$	1.908
F. Partially hydroxylated (110) D-layer, E_{vdw} = 8.4 kcal	
None $O_{carbonyl}$–$O_{surface}$	>2.40
None $O_{carbonyl}$–$Al_{surface}$	>2.40
None $C_{carbonyl}$–$O_{surface}$	>2.40
None $C_{carbonyl}$–$Al_{surface}$	>2.40

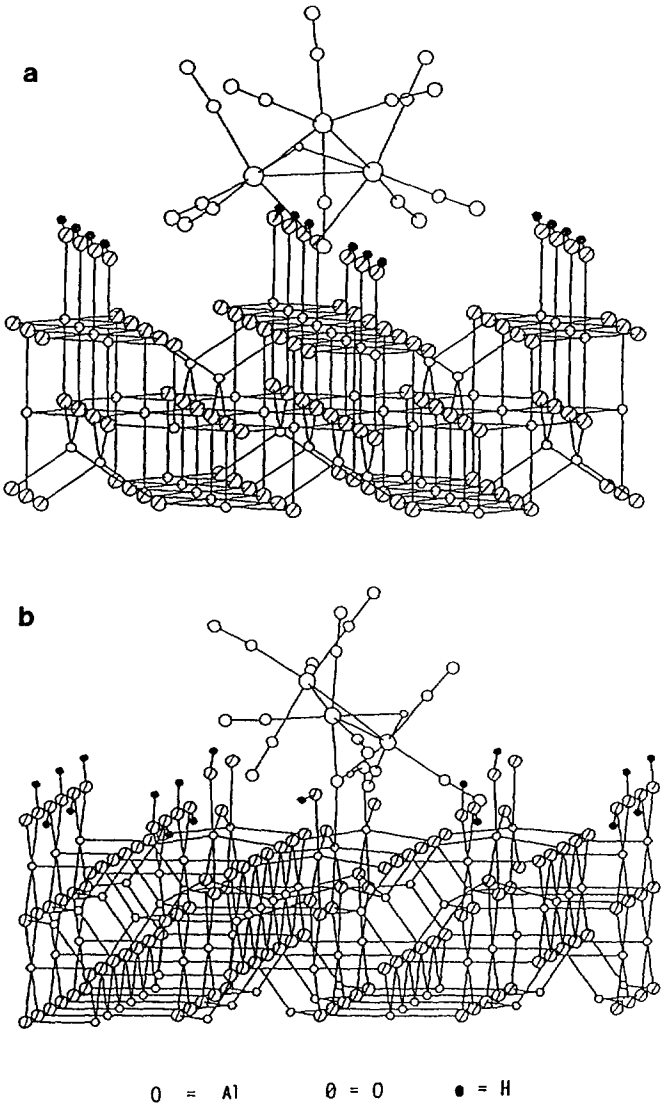

FIG. 10. Models for $(\mu\text{-H})(\mu\text{-OAl}\equiv)Os_3(CO)_{10}$ with $(\mu\text{-H})Os_3(CO)_{10}$ bound to a surface oxygen of (a) the partially hydroxylated (100) plane of γ-alumina and (b) the partially hydroxylated (110) D-layer of γ-alumina.

The calculated van der Waals interaction energy is 8.4 kcal. In the relaxation procedure the Os(2)$(CO)_3$ unit was rotated 3° and one of the carbonyl groups was bent 5° from linear.

D. Modeling the $(\mu\text{-OAl}\equiv)_2Os_3(CO)_{10}$ Surface Complex

Table 4 shows that $Os_3(CO)_{10}$ cannot be fitted with a double oxygen bridge to the following local regions of γ-alumina: fully hydroxylated (100) face, fully hydroxylated C-layer of the (110) face, and fully hydroxylated D-layer of the (110) face. Calculated minimum van der Waals energies are 3113.4, 8794.0, and 5357.3 kcal, respectively. A number of unreasonably "short" nonbonded contacts are observed between cluster and surface atoms.

TABLE 4

Van der Waals Energies and Short Nonbonded Distances between $Os_3(CO)_{10}$ and Local Regions of Alumina Surface

Number of short contacts	Range of short contacts (Å)
A. Fully hydroxylated (100) plane, E_{vdw} = 3113.4 kcal	
11 $O_{carbonyl}$–$O_{surface}$	1.073–2.376
4 $O_{carbonyl}$–$Al_{surface}$	1.252–1.658
12 $C_{carbonyl}$–$O_{surface}$	1.157–2.046
4 $C_{carbonyl}$–$Al_{surface}$	1.500–1.831
3 $Os_{cluster}$–$O_{surface}$	1.827–1.927
B. Fully hydroxylated (110) C-layer, E_{vdw} = 8794.0 kcal	
11 $O_{carbonyl}$–$O_{surface}$	1.255–2.257
3 $O_{carbonyl}$–$Al_{surface}$	0.755–1.793
8 $C_{carbonyl}$–$O_{surface}$	0.333–2.162
3 $C_{carbonyl}$–$Al_{surface}$	1.381–1.927
C. Fully hydroxylated (110) D-layer, E_{vdw} = 5357.3 kcal	
10 $O_{carbonyl}$–$O_{surface}$	1.287–2.210
3 $O_{carbonyl}$–$Al_{surface}$	1.003–1.845
10 $C_{carbonyl}$–$O_{surface}$	0.550–2.432
2 $C_{carbonyl}$–$Al_{surface}$	1.424–1.558

For the local regions of γ-alumina derived from partially hydroxylated (100) face and partially hydroxylated (110) face C-layer, and partially hydroxylated (110) face D-layer, the $Os_3(CO)_{10}$ fragment could not be fitted with a double-oxygen bridge because of the long distance between available oxygen atoms, >5 Å, compared with the observed distance between the bridge oxygen atoms, 2.59 Å, in the model compound $(\mu\text{-OMe})_2Os_3(CO)_{10}$.

The fragment $Os_3(CO)_{10}$ could not be fitted to any of the defect sites of alumina surface and still retain the double-bridged arrangement of oxygen atoms.

IV. SUMMARY AND CONCLUSIONS

Based on descriptions of local regions of hydroxylated silica and alumina surfaces (9–13), we have derived physical models for these surfaces using computer graphics techniques. These models, while simplistic, represent an advance in visualizing possible arrangements of surface hydroxyl groups and also surface oxygens in dehydroxylated regions. In turn, these models can provide insight as to how organometallic species might be accommodated on the various surface sites. Thus we find that these models favor singly oxygen-bridged surface complexes $(\mu\text{-H})(\mu\text{-OSi}\equiv)Os_3(CO)_{10}$ and $(\mu\text{-H})(\mu\text{-OAl}\equiv)Os_3(CO)_{10}$ over doubly oxygen bridged complexes $(\mu\text{-OSi}\equiv)_2Os_3(CO)_{10}$ and $(\mu\text{-Al}\equiv)_2Os_3(CO)_{10}$ in accord with the preponderance of experimental data (2–7), in particular solid-

state ^{13}C NMR data (6) for the cluster on silica and more recent EXAFS data for the cluster on γ-alumina (3e). Additionally, these models distinguish between the most favorable and least favorable local sites that will accommodate the singly oxygen-bridged surface complexes. Although relaxation of the cluster $(\mu\text{-H})Os_3(CO)_{10}$ is required to achieve a "good fit" in several cases, the extent of relaxation involves little distortion of the cluster from its structure in the model compound $(\mu\text{-H})(\mu\text{-OSiEt}_3)Os_3(CO)_{10}$ (24). Doubly oxygen-bridged arrangements $(\mu\text{-OSi}\equiv)_2Os_3(CO)_{10}$ and $(\mu\text{-OAl}\equiv)_2Os_3(CO)_{10}$ do not appear to be readily accommodated on any of the local surface regions of silica or alumina without extreme distortion of the surface and or the cluster.

Conclusions drawn from this study are in agreement with spectroscopic and analytical studies (2–7). These two examples illustrate the potential for the application of modeling techniques to surface organometallic chemistry. Such techniques can be useful in gaining insight into the potential properties of surface substrates in interacting with multimetallic species.

ACKNOWLEDGMENTS

Support from NATO to S.G.S. and J.M.B. and support to S.G.S. from the National Science Foundation through Grant CHE-91-04035 are gratefully acknowledged.

REFERENCES

1. See, for example, (a) Basset, J. M., and Choplin, A., *J. Mol. Catal.* **21,** 95 (1983); (b) Psaro, R., and Ugo, R., *in* "Metal Clusters and Catalysis" (B. C. Gates, L. Guczi, and H. Knözinger, Eds.), p. 451, Elsevier, Amsterdam, 1986; (c) Evans, J., *in* "Surface Organometallic Chemistry: Molecular Approaches to Surface Catalysis" (J. M. Basset, B. C. Gates, J. P. Candy, A. Choplin, F. Quignard, N. Leconte, and C. Santini, Eds.), p. 47, Kluwer, Dordrecht, 1988; (d) Basset, J. M., Candy, J. P., Choplin, A., Santini, C., and Theolier, A., *Catal. Today* **6,** 1 (1989); (e) Iwasawa, Y., and Gates, B. C., *Chemtech* **3,** 173 (1989); (f) Yermakov, Y. I., Kuznetsov, B. N., and Zakharov, V. A., "Catalysis by Supported Complexes," Elsevier, Amsterdam, 1981; (g) Schwartz, J., *Acc. Chem. Res.* **18,** 302 (1985); (h) Lamb, H., Gates, B. C., and Knözinger, H., *Angew. Chem. Int. Ed. Engl.* **27,** 1127 (1988); (i) Psaro, R., Dossi, C., Fiso, A., and Ugo, R., *Res. Chem. Intermed.* **15**(1), 31 (1991).
2. (a) Besson, B., Moraweck, B., Smith, A. K., Basset, J. M., Psaro, R., Fusi, A., and Ugo, R., *J. Organomet. Chem.* **192,** C30 (1980); (b) Psaro, R., Ugo, R., Zanderighi, G. M., Besson, B., Smith, A. K., and Basset, J. M., *J. Organomet. Chem.* **213,** 215 (1981); (c) Besson, B., Choplin, A., D'Ornelas, L., and Basset, J. M., *J. Chem. Soc. Chem. Commun.*, 843 (1982); (d) Basset, J. M., Besson, B., Choplin, A., and Theolier, A., *Philos. Trans. R. Soc. London Ser. A* **308,** 115 (1982); (f) Choplin, A., Besson, B., D'Ornelas, L., Sanchez-Delgado, R., and Basset, J. M., *J. Am. Chem. Soc.* **110,** 2783 (1988).
3. (a) Deeba, M., and Gates, B. C., *J. Catal.* **67,** 303 (1981); (b) Knözinger, H., and Zhao, Y., *J. Catal.* **71,** 337 (1981); (c) Deeba, M., Streusand, M. J., Schrader, G. L., and Gates, B. C., *J. Catal.* **69,** 218 (1981); (d) Barth, R., Gates, B. C., Zhao, Y., Knözinger, H., and Hulse, J., *J. Catal.* **82,** 147 (1983); (e) Duivenvoorden, F. B. M., Koningsberger, D. C., Uh, Y. S., and Gates, B. C., *J. Am. Chem. Soc.* **108,** 6254 (1986).
4. Knözinger, H., Zhao, Y., Tesche, B., Barth, R. Epstein, R., Gates, B. C., and Scott, J. P., *Faraday Discuss.* **72,** 53 (1981).
5. (a) Cook, S. L., Evans, J., and Greaves, G. N., *J. Chem. Soc. Chem. Commun.*, 1287 (1983); (b) Cook, S. L., Evans, J., McNulty, G. S., and Greaves, G. N., *J. Chem. Soc. Dalton Trans.*, 7 (1986); (c) Alexiev, V. D., Binsted, N., Evans, J., Greaves, G. N., and Price, R. J., *J. Chem. Soc. Chem. Commun.*, 395 (1987).
6. (a) Walter, T. H., Frauenhoff, G. R., Shapley, J. R., and Oldfield, E., *Inorg. Chem.* **27,** 2563 (1988); (b) Walter, T. H., Frauenhoff, G. R., Shapley, J. R., and Oldfield, E., *Inorg. Chem.* **30,** 4732 (1991).
7. (a) Dossi, C., Psaro, R., Zanoni, R., and Stone, F. S., *Spectrochim. Acta Part A* **43,** 1507 (1987); (b) Dossi, C., Fusi, A., Grilli, E., Psaro, R., Ugo, R., and Zanoni, R., *Catal. Today* **2,** 585 (1988); (c) Dossi, C., Fusi, A., Psaro, R., and Zanderighi, G. M., *Appl. Catal.* **46,** 145 (1989).
8. Hsu, L.-Y., Shore, S. G., D'Ornelas, L., Choplin, A., and Basset, J. M., *Polyhedron* **7,** 2399 (1988).
9. (a) Krejei, I., and Ott, E., *J. Phys. Chem.* **35,** 2061 (1931); (b) Frondel, P. C., "The System of Minerology of Dana," 7th ed., Vol. 3 (Silica Minerals), p. 154, John Wiley, New York, 1962; (c) Iler, R. K., "The Colloid Chemistry of Silica and Silicates," pp. 242–247, Cornell University Press, Ithaca, NY, 1955.
10. (a) Armistead, C. G., Tyler, A. J., Hambleton, F. H., Mitchell, S. A., and Hokey, J. A., *J. Phys. Chem.* **73,** 3947 (1969); (b) Sindorf, D. W., and Maciel, G. E., *J. Phys. Chem.* **86,** 5208 (1982); (c) Sindorf, D. W., and Maciel, G. E., *J. Am. Chem. Soc.* **105,** 1487 (1983); (d) Chuang, I.-S., Kinney, D. R., Bronnimann, C. E., Ziegler, R. C., and Maciel, G. E., *J. Phys. Chem.* **96,** 4027 (1992).
11. (a) Peri, J. B., and Helmsley, A. L., Jr., *J. Phys. Chem.* **72,** 1926 (1968); (b) van Boosmalen, A. J. and Mol, J. C., *J. Phys. Chem.* **82,** 2748 (1978). (c) Ghiotti, G., Garrone, E. Mortera, C., and Boccuzi, C., *J. Phys. Chem.* **83,** 2863 (1979); (d) Sindorf, D. W., and Maciel, G. E., *J. Phys. Chem.* **87,** 5516 (1983).
12. (a) Welberry, T. R., Hua, G. L., and Withers, R. L., *J. Appl. Crystallogr.* **22,** 87 (1989); (b) Hua, G. L., Welberry, T. R., Withers, R. L., and Thompson, J. G., *J. Appl. Crystallogr.* **21,** 458 (1988).
13. (a) Wyckoff, R. W. G., "Crystal Structure," Vol. 1, p. 318, Interscience, New York, 1963; (b) Wyckoff, R. W. G., *Am. J. Sci.* **9,** 448 (1925); (c) Wyckoff, R. W. G., *Z. Kristallogr.* **62,** 189 (1925).
14. Created by E. K. Davies, Chemical Crystallography Laboratory, Oxford University, and distributed by Chemical Design Ltd., Oxford, England.
15. The 1986 version of MacroModel was provided by Professor Clark still, Department of Chemistry, Columbia University.
16. (a) Wells, A. F., "Structural Inorganic Chemistry," 5th ed., p. 1011, Clarendon Press, Oxford, England, 1984; (b) Smolin, Y. I., Shepelev, Y. F., and Titov, A. Pv., *Phys. Crystallogr.* **17,** 749 (1973); (c) Cruickshank, D. W. J., Lynton, H., and Barclay, G. A., *Acta Crystallogr.* **15,** 491 (1962); (d) Howie, A. R., and West, A. R., *Acta Crystallogr. Sect. B* **33,** 381 (1977).
17. (a) Lippens, B. C., and Boer, J. H., *Acta Crystallogr.* **17,** 1312 (1964); (b) Lippens, B. C., Ph.D. thesis, Delft, Holland, 1961.
18. Coordinates for γ-alumina were deduced from Lippens' work (17) prior to more recent results of Zhou and Snyder. The overall structures from these two studies are equivalent. Differences in Al–O distances in these structures are small and are not significant with respect to the criteria employed for deciding how well a cluster is accommodated on a surface site. Zhou, R.-S., and Snyder, R. L., *Acta Crystallogr. Sect. B* **47,** 617 (1991).
19. Knozinger, H., and Ratnasamy, X., *Catal. Rev.* **17,** 31 (1978).
20. Knozinger, H., *Adv. Catal.* **25,** 184 (1976).
21. Cornelius, E. B., Milliken, T. H., Mills, G. A., and Oblad, A. G., *J. Phys. Chem.* **59,** 809 (1955).

22. Peri, J. B., *J. Phys. Chem.* **69,** 220 (1965).
23. Verwey, E. J. W., *Z. Kristallogr.* **91,** 65 (1935).
24. D'Ornelas, L., Choplin, A., Basset, J. M., Hsu, L.-Y., and Shore, S. G., *Nouv. J. Chim.* **9,** 155 (1985).
25. Churchill, M. R., and Wasserman, H. J., *Inorg. Chem.* **19,** 2391 (1980).
26. Allinger, N. L., and Yuh, Y. H., Force field of MM2 Program, 1980.
27. We estimated ε and r^* for Al and Os by extrapolation: (a) van der Waals parameters of MM2 and MMP2 (1985); (b) Brubaker, G. R., and Johnson, D. W., *Coord. Chem. Rev.* **53,** 1 (1984); (c) Catlow, C. R. A., and Cormack, A. N., *Acta Crystallogr. Sect. B* **40,** 195 (1984).